Dissection of the Golgi Complex. I. Monensin Inhibits the Transport of Viral Membrane Proteins from *Medial* to *Trans* Golgi Cisternae in Baby Hamster Kidney Cells Infected with Semliki Forest Virus

GARETH GRIFFITHS, PAUL QUINN, and GRAHAM WARREN
European Molecular Biology Laboratory, 6900 Heidelberg, Federal Republic of Germany

ABSTRACT Baby hamster kidney (BHK) cells were infected with Semliki Forest virus (SFV) and, 2 h later, were treated for 4 h with 10 μM monensin. Each of the four to six flattened cisternae in the Golgi stack became swollen and separated from the others. Intracellular transport of the viral membrane proteins was almost completely inhibited, but their synthesis continued and they accumulated in the swollen Golgi cisternae before the monensin block. In consequence, these cisternae bound large numbers of viral nucleocapsids and were easily distinguished from other swollen cisternae such as those after the block. These intracellular capsid-binding membranes (ICBMs) were not stained by cytochemical markers for endoplasmic reticulum (ER) (glucose-6-phosphatase) or *trans* Golgi cisternae (thiamine pyrophosphatase, acid phosphatase) but were labeled by *Ricinus communis* agglutinin I (RCA) in thin, frozen sections. Since this lectin labels only Golgi cisternae in the middle and on the *trans* side of the stack (Griffiths, G., R. Brands, B. Burke, D. Louvard, and G. Warren, 1982, *J. Cell Biol.*, 95:781-792), we conclude that ICBMs are derived from Golgi cisternae in the middle of the stack, which we term *medial* cisternae. The overall movement of viral membrane proteins appears to be from *cis* to *trans* Golgi cisternae (see reference above), so monensin would block movement from *medial* to the *trans* cisternae. It also blocked the trimming of the high-mannose oligosaccharides bound to the viral membrane proteins and their conversion to complex oligosaccharides. These functions presumably reside in *trans* Golgi cisternae. This is supported by data in the accompanying paper, in which we also show that fatty acids are covalently attached to the viral membrane proteins in the *cis* or *medial* cisternae. We suggest that the Golgi stack can be divided into three functionally distinct compartments, each comprising one or two cisternae. The viral membrane proteins, after leaving the ER, would all pass in sequence from the *cis* to the *medial* to the *trans* compartment.

As viral membrane proteins are transported from their site of synthesis in the rough endoplasmic reticulum (ER) to the cell surface, they pass through the stacks of flattened cisternae that constitute the central feature of the Golgi complex (3, 5). The mechanism of transport and precise route taken through the Golgi stack are still unknown, but transport is accompanied by a precise sequence of structural changes in the transported protein and its attached oligosaccharides (10–12, 15, 18, 25, 31, 34). If these changes reflect the movement of proteins from one part of the stack to another, it would be important to determine precisely where these changes occur. We would then gain a better understanding of how the Golgi stack functions.

One approach which was very useful in early metabolic studies was to block the pathway with a specific inhibitor (see e.g. 16). The intermediate before the block accumulated and could then be isolated and characterized. For the intracellular transport pathway, an equivalent inhibitor would cause the transported protein to accumulate in the membrane compartment before the block. If this membrane compartment could then be isolated, or at least distinguished, from other membrane compartments, the structural changes in the transported proteins could be related to the precise point reached on the

THE JOURNAL OF CELL BIOLOGY · VOLUME 96 MARCH 1983 835-850

intracellular transport pathway. Unfortunately, most of the inhibitors of intracellular transport also inhibit protein synthesis so that no protein accumulates. There are, however, exceptions, the most useful being the Na^+ ionophores of which monensin is an example (26). It blocks transport at some point in the Golgi complex but has no significant effect on protein synthesis (37, 38). It has previously proven difficult to locate the precise site of the block because monensin destroys the characteristic morphology of the Golgi stacks; the flattened cisternae become swollen and separated from each other.

Johnson and Schlessinger (13) noted that cells infected with Sindbis virus and then treated with monensin contained a class of swollen Golgi cisternae that were covered by viral nucleocapsids. They suggested that these were intermediates on the transport pathway. It occurred to us that these structures were in fact the membrane compartment before the monensin block. The viral membrane proteins were accumulating there and in consequence the membranes bound viral nucleocapsids, a process that would normally occur only at the plasma membrane. It no longer mattered that monensin disrupted the typical Golgi morphology; the bound nucleocapsids clearly distinguished these Golgi cisternae from others in the stack.

Using this fortuitous observation, we set out to identify the site at which monensin blocks transport. We have used Semliki Forest virus (SFV), a virus closely related to Sindbis, which is affected in a similar way by monensin (14). Using a combination of cytochemistry, immunocytochemistry, and biochemistry, we have been able to determine the site within the Golgi stack at which monensin blocks transport of the viral membrane proteins.

MATERIALS AND METHODS

Cells, Virus, and Monensin: Baby hamster kidney (BHK)-21 cells and the RiC^R-14 line derived from it (19) were grown and infected with SFV as described previously (5, 8). They were normally used 6 h after infection.

Monensin (Eli Lilly, Indianapolis, IN) was stored as a 10 mM solution in absolute ethanol at −80°C for up to 3 mo. It was diluted directly into the medium used to bathe the cells. Uninfected BHK cells were treated for 4 h with 10 μM monensin. Infected BHK cells were treated in the same way but the drug was added 2 h after the start of infection.

Labeling Studies: Labeling with ^{35}S-methionine, [^3H]mannose, and the preparation of labeled oligosaccharides were performed as described previously (5).

Electron Microscopy: The techniques for preparing cells for electron microscopy, both for conventional Epon embedding and for frozen section immunocytochemistry, including double-labeling experiments, have been described previously (5, 8, 9).

Quantitation of Double-labeling Experiments: Thin, frozen sections of infected BHK cells, with and without monensin treatment, were labeled with anti-spike protein antibodies and *Ricinus communis* agglutinin I (RCA) and anti-RCA antibodies. These antibodies were then visualized using protein A conjugated to either 5- or 12-nm colloidal gold particles. The radius of a virus particle was ~225 Å (excluding the spike proteins which were normally not visible in frozen sections), and both sizes of gold were found within 250 Å of the membrane of budding or budded virus. Hence, all gold particles within 500 Å of the center of the virus were counted as labeling the viral profile. When groups of viral profiles were found, the total number of gold particles found within the overlapping 1,000-Å diameter circles was averaged over the number of viral particles seen. Such groups were regarded as a single count for data analysis. Results were expressed as gold particles per viral profile plus-or-minus standard deviation of the mean.

Cytochemistry: For all cytochemical preparations the cells were fixed in 0.5% glutaraldehyde in 100 mM PIPES, pH 7.0, containing 5% (wt/vol) sucrose for 30 min, washed in the same buffer containing 10% (wt/vol) sucrose, and then briefly washed in the buffer used for the subsequent cytochemical incubation.

GLUCOSE 6-PHOSPHATASE: The procedure used was a slight modification of that developed by Wachstein and Meisel (40). The medium was made up by dissolving 0.19 gm of glucose-6-phosphate (Sigma Chemical Co., St. Louis, MO) in 10 ml of 80 mM Tris-maleate buffer, pH 6.5, and then slowly adding 80 μl of a 12% (wt/vol) solution of lead nitrate. The optimal incubation time was 120 min at room temperature. Control incubations were without substrate.

THIAMINE PYROPHOSPHATASE: This was the standard method of Novikoff and Goldfisher (22). To 10 ml of 80 mM Tris-maleate buffer, pH 7.2, 9 mg of thiamine pyrophosphate (HCl salt; Sigma Chemical Co.) was added, followed by 50 μl of 1M $MnCl_2$ and then, slowly, 80 μl of a 12% (wt/vol) lead nitrate solution. Optimal incubation time was 45 min at 37°C. Control incubations were without substrate.

ACID PHOSPHATASE: The incubation medium was the same as that used previously (7). To 25 ml of 50 mM sodium acetate buffer, pH 5.0, 0.25 ml of 12% (wt/vol) lead nitrate solution was added and then, slowly, 2.5 ml of a 3% (wt/vol) glycerophosphate (Sigma Chemical Co.) solution. Optimal incubation time was 45 min at 37°C. Control incubations were either without substrate or with the addition of 10 mM NaF.

NICOTINAMIDE ADENINE DINUCLEOTIDE PHOSPHATASE: This was assayed as described by Smith (33). The incubation mixture consisted of 1–2 mM nicotinamide adenine dinucleotide phosphate (NADP) (Sigma Chemical Co.), 40 mM sodium acetate buffer, pH 5.0, 4 mM lead acetate, and 5% (wt/vol) sucrose. Incubation times from 30 min to 3 h at 37°C were used. Control incubations were carried out without substrate.

Post-incubation Processing: After incubation the cells, still on the petri dishes, were washed for 5 min in the buffer used for the cytochemical incubation and then briefly in 80 mM sodium cacodylate, pH 7.2, followed by 2% (wt/vol) osmium tetroxide solution in 80 mM sodium cacodylate for 15 min at room temperature. Following three brief rinses in the cacodylate buffer, the cells were dehydrated in ethanol and the monolayer was brought off the dish using propylene oxide (8) and embedded in Epon 812.

RESULTS

Intracellular Capsid-binding Membranes Appear in Infected Cells Treated with Monensin

A cross-section through the peri-nuclear region of a BHK cell revealed the typical organization of the Golgi complex.

FIGURES 1–4 Fig. 1: Epon section of part of the perinuclear region of a BHK cell adjacent to the plasma membrane (*PM*). Seven Golgi stacks (arrowheads) are visible in this micrograph, each comprising four to six cisternae. The *ER* is also apparent, often in close proximity to the stacks. The long arrow indicates contiguity between *ER* and a Golgi stack. Between the plasma membrane and the plastic layer (*Pl*), which comes off the petri dish with propylene oxide, is extracellular electron-dense material often apparent after tannic acid treatment. This treatment also makes it difficult to see the ribosomes. (*N*), Nucleus. × 28,000. All bars in microns. Fig. 2: Epon section of part of a BHK cell infected with Semliki Forest Virus (*SFV*). Two typical Golgi stacks are indicated (*G*) as well as endoplasmic reticulum. At the *PM* a budding virion is indicated (*BV*), as well as a complete virion (*V*) in the extracellular space between the plasma membrane and the plastic layer (*Pl*). In the cytoplasm a number of capsid structures (*CS*) are apparent. These are dense, vesicular structures with many nucleocapsids (*C*) on their surface (see references 1, 8). The asterisks denote vacuoles containing bound nucleocapsids on their surface. These are occasionally found in infected cells and resemble the ICBMs found after monensin treatment (see Figs. 4 and 5). × 47,000. Fig. 3: Part of the perinuclear region of a BHK cell after treatment with 10 μM monensin. Large numbers of vacuoles (*v*) and smaller vesicles are evident in the region normally occupied by the Golgi complex. The endoplasmic reticulum (arrowheads) appears normal but mitochondria (*M*) are typically electron-dense. × 9,100. Fig. 4: Part of the perinuclear region of an SFV-infected BHK cell after treatment with 10 μM monensin. The asterisks indicate typical ICBM vacuoles which are found extensively in the Golgi region of the cell. These vacuoles are covered with nucleocapsids on their outside and often contain budded and budding virus inside. In addition, a number of smooth vacuoles are evident. Mitochondria (*M*) appear abnormal but *ER* (arrowheads) is not noticeably affected by the drug. × 25,000.

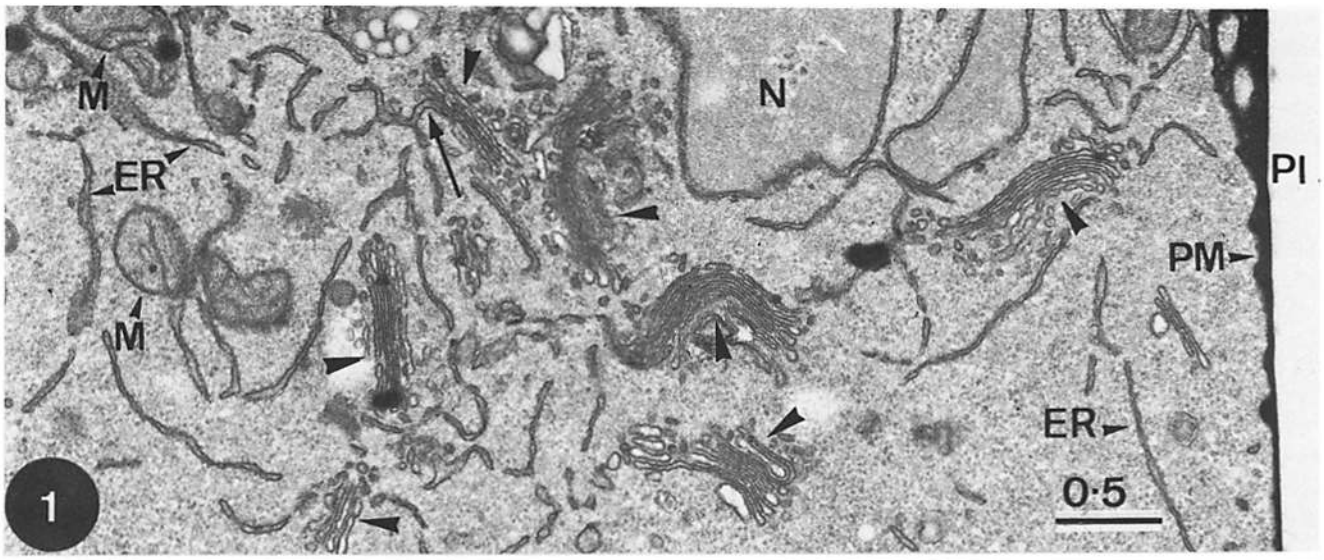
M
ER
M
N
PI
PM
ER
0·5
1

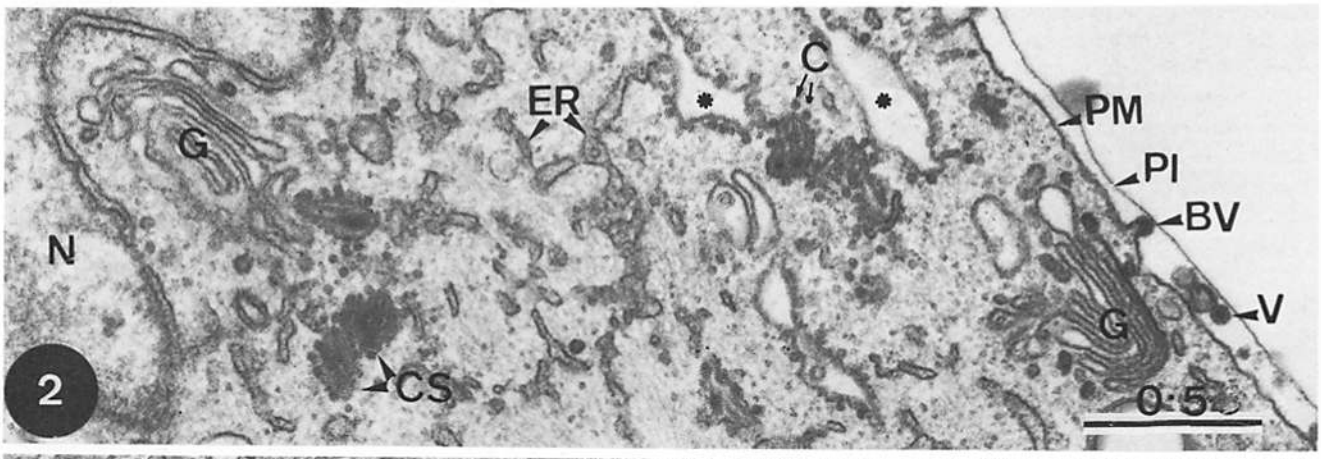
G
N
ER
C
PM
PI
BV
V
G
CS
0·5
2

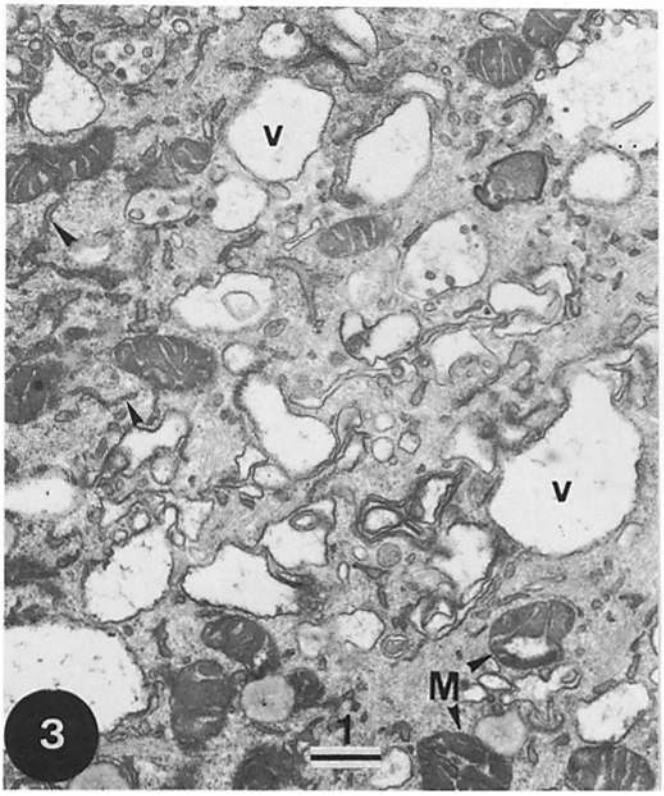
v
v
M
1
3

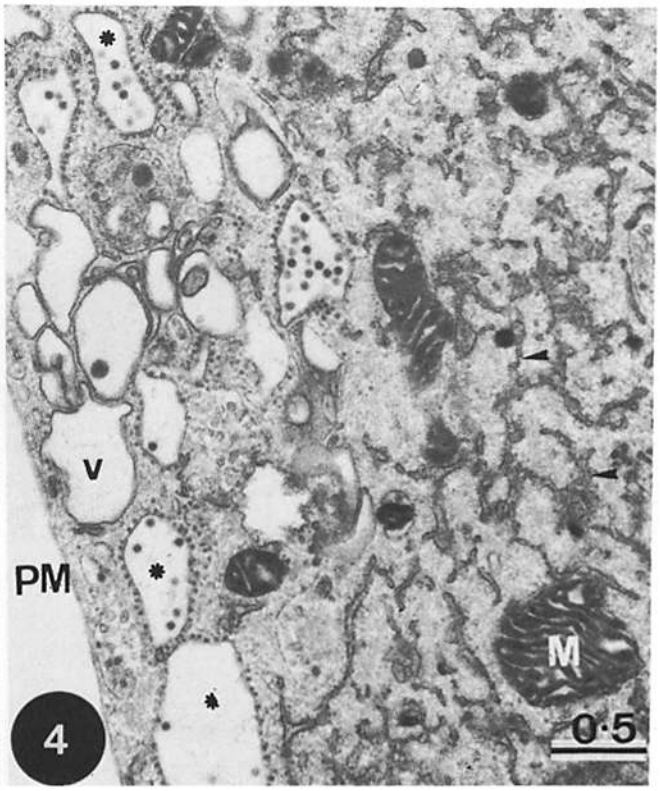
v
PM
M
0·5
4

The central feature, the Golgi stack, comprised four to six flattened cisternae that were slightly dilated at their rims and were closely apposed to each other (Fig. 1). In this, as in other cells and tissues (13, 14, 28, 35, 37–39), monensin had a dramatic effect on the morphology of the Golgi complex. After 4 h of treatment with 10 μM monensin, the Golgi stacks were no longer visible. They were replaced by large vacuoles (see Fig. 3) which appeared to arise by extensive swelling of the individual Golgi cisternae. Though these swollen cisternae were still restricted to a peri-nuclear region, they were no longer closely apposed. The morphology of other cellular structures was largely unaltered by the presence of monensin, except that the mitochondrial matrices appeared to be more electron-dense (cf. Figs. 1 and 3).

When BHK cells were infected with SFV and the cells were examined 4–6 h later, there was no significant change in their overall morphology. The structure of the Golgi stacks, in particular, was the same as in uninfected cells (cf. Figs. 1 and 2). There were, however, two additional features. The first was the presence of capsid structures, first described by Acheson and Tamm (1), but for which no function is known (see reference 8). The second feature was the appearance of budding virus at the plasma membrane (Fig. 2). Cells infected with SFV for 2 h were then treated with monensin for 4 h. This treatment is known to block the intracellular transport of the SFV membrane proteins (14), and only rarely was virus seen to bud from the plasma membrane (Fig. 4; and see Fig. 25). The Golgi cisternae were swollen as in uninfected cells treated with monensin, but in this case two distinct types of swollen cisternae could be seen (Fig. 4). The first type was smooth-surfaced and indistinguishable from those seen in uninfected cells treated with monensin (cf. Figs. 3 and 4). The second type was covered by viral nucleocapsids, and completed viral particles were frequently found inside (Fig. 4). In many cases, it was even possible to see virus budding into their interior (Fig. 5). To distinguish these swollen cisternae from those that are smooth-surfaced, and because of their capsid-binding properties, we have chosen to call them "intracellular capsid-binding membranes" (ICBMs).

ICBMs Contain High Concentrations of Viral Membrane Proteins

Thin, frozen sections of infected BHK cells were labeled with antibody to the viral membrane proteins followed by protein A–gold. We have previously shown (5) that the ER and Golgi complex membranes are uniformly labeled with this antibody, and an example is presented in Fig. 6. With more observations, it has also become apparent that there is a significant amount of smooth ER (SER) in these cells (Fig. 6) which is continuous with rough ER (RER) (not shown). This structure also labels with the antibody, as do virions budding at the plasma membrane, and capsid structures, which have been described earlier (1, 8; and Fig. 6). After treatment with 10 μM monensin for 4 h, the level of labeling of the plasma membrane was reduced considerably and very few budding

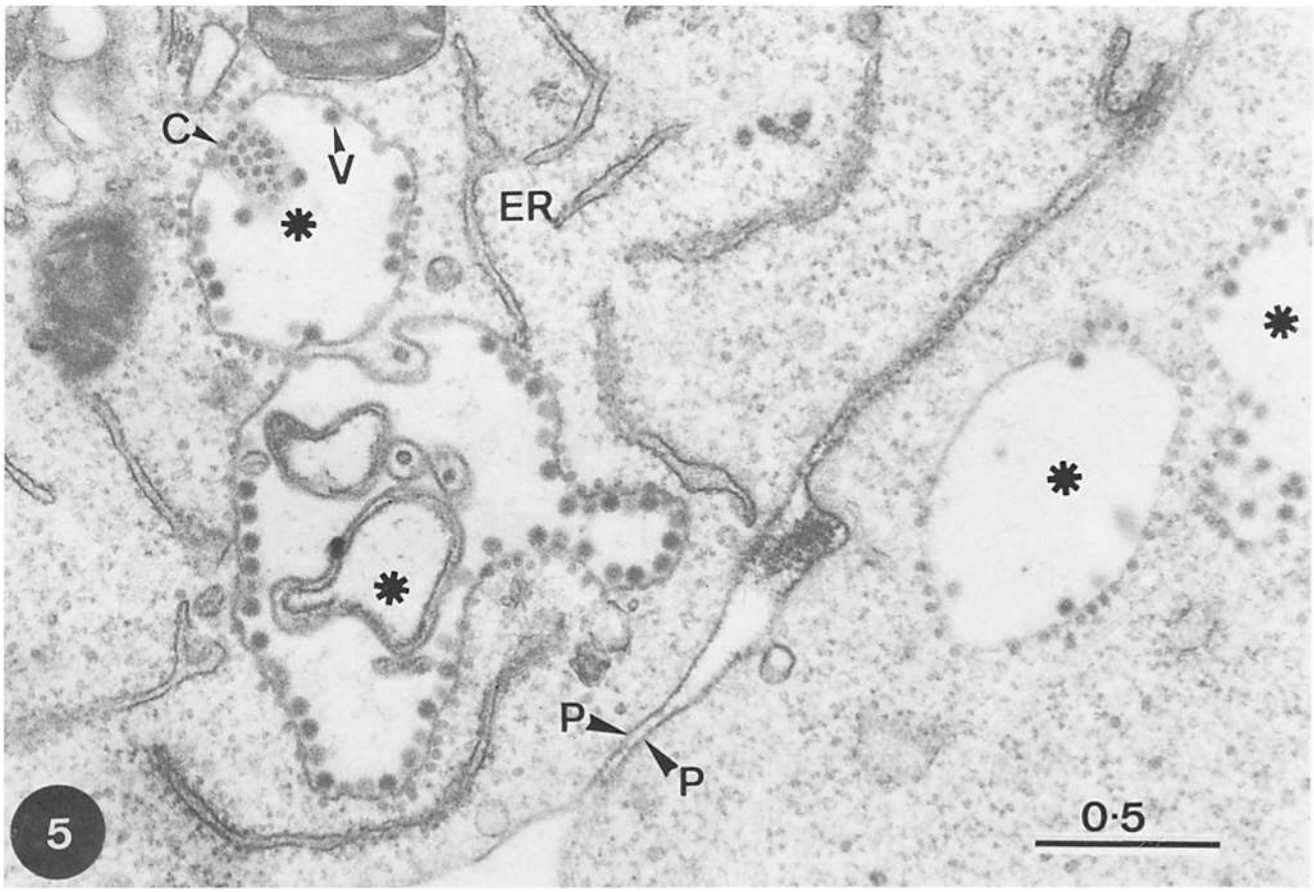

FIGURE 5 Image of parts of two adjacent BHK cells (P, plasma membrane) at high magnification, showing four ICBMs (asterisks). Variable numbers of nucleocapsids (C) are seen on the outside of these vacuoles, and in the upper left corner of the micrograph these can be seen in face view since the section has cut the vacuole obliquely. On the inside of the ICBM are large numbers of budded virions, with the spike structure apparent in many of these (e.g., *V*).

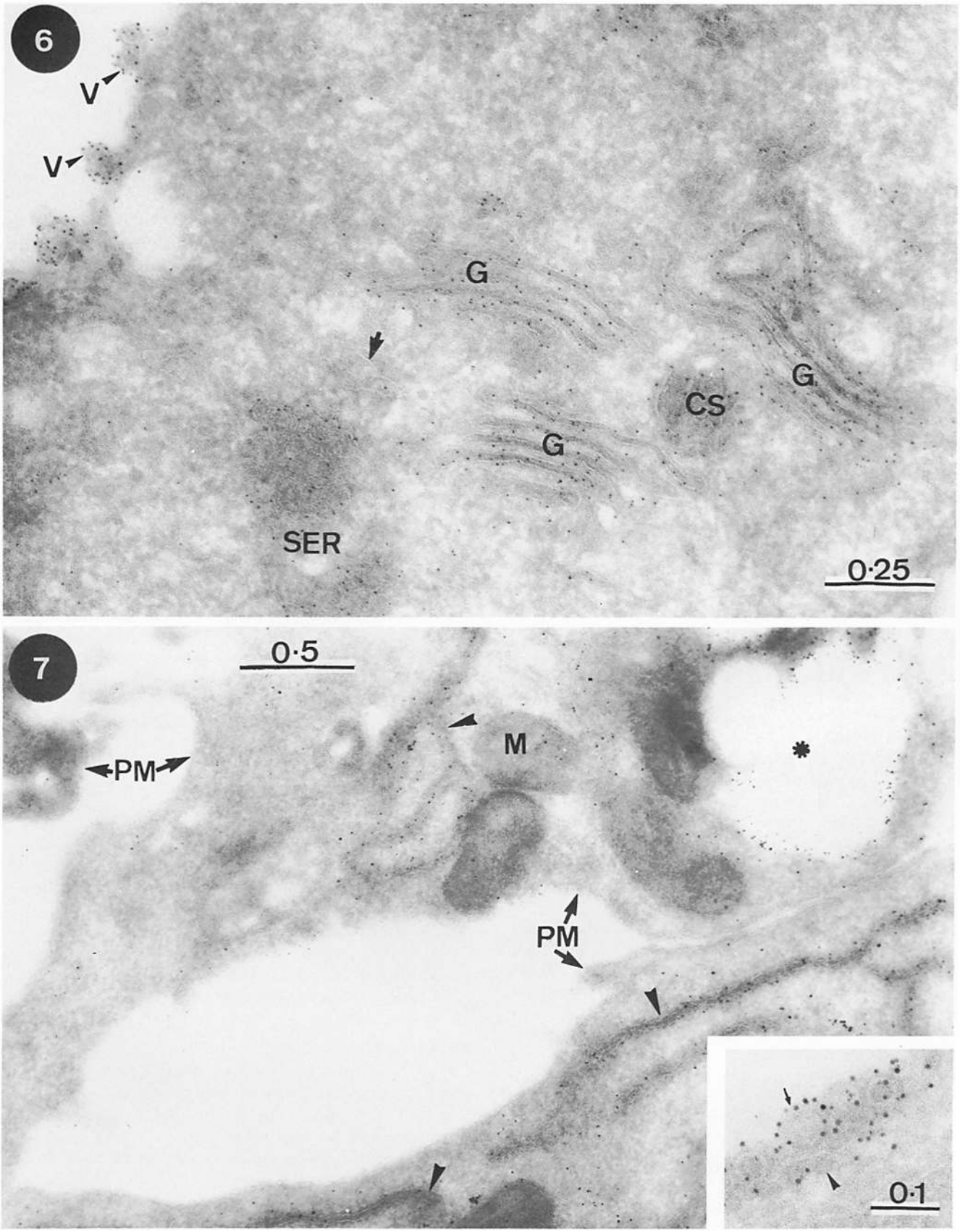

FIGURES 6 and 7 Fig. 6: Frozen thin section of an SFV-infected BHK cell immunolabeled with an affinity-purified antibody against the virus spike proteins followed by protein A–gold. Extensive labeling is seen over three Golgi stacks (*G*) as well as over smooth ER (*SER*). The labeling of rough ER (arrow) is always considerably less than that of the *SER*. At the plasma membrane, labeled budding virions (*V*) are indicated. × 80,000. Fig. 7: Frozen thin section of monensin-treated, SFV-infected BHK cells labeled with anti-spike protein antibodies. There is no significant labeling of the plasma membrane but extensive labeling of ER (arrowheads) and the inside of a large ICBM (asterisk). The *inset* shows, at higher magnification, detail of the labeling of this ICBM. The arrow indicates a budding virion and the arrowhead indicates a nucleocapsid on the cytoplasmic side of the vacuole. × 42,000. *Inset*, × 124,000.

profiles were seen (Fig. 7; and see Fig. 25). The labeling of the whole ER appeared to be higher than that seen in untreated infected cells. ICBMs were heavily labeled (Fig. 7, *inset*), the density of labeling being much higher than that seen in the Golgi membranes of infected cells not treated with monensin. Smooth-surfaced vacuoles of unknown origin were labeled, but the level of labeling was much less than that of ICBMs (see Fig. 27).

ICBMs ARE DERIVED FROM GOLGI CISTERNAE IN THE MIDDLE OF THE STACK

Cytochemical Studies

GLUCOSE-6-PHOSPHATASE (G-6-Pase): This is a marker for the whole of the ER. Although there is extensive biochemical evidence showing significant G-6-Pase activity in "pure" isolated Golgi fractions from liver (20), there has been no convincing cytochemical demonstration of the enzyme in Golgi cisternae in vivo (20, 35). It has, however, been found in the liver subfraction GF3 that is believed to correspond to *cis* Golgi cisternae (4).

We consistently found the cytochemical reaction product dispersed throughout the ER of BHK cells, before and after infection. The great majority of the ER in these cells is RER which is continuous with the outer nuclear membrane. As mentioned above, there is some SER whose structure is very distinct and is identical to that seen in liver (unpublished data). Both reacted uniformly for G-6-Pase. In our preparations we consistently found that the major part of the Golgi stack had no significant amounts of reaction product. However, as is clear from Fig. 8, areas of reactive ER were closely apposed to one (and very occasionally to both) side(s) of the Golgi stack. Because the ribosomes on the RER are not usually visible in these cytochemical preparations, it is very difficult to distinguish between ER, transitional elements of the ER, and the first true *cis* cisterna of the Golgi complex (23). Thus an image such as Fig. 9 might be interpreted as having reaction product in the first (*cis*) cisterna of the stack, or in the ER closely apposed to this Golgi cisterna. As we have pointed out before (8), one cannot easily distinguish the *cis* from the *trans* side of the Golgi complex in BHK cells by morphological criteria alone. What is important for this paper is that G-6-Pase activity was localized in the whole ER and possibly the first *cis*-cisterna but that the rest of the stack was unreactive.

Fig. 10 shows a BHK cell treated with 10 μM monensin and incubated for G-6-Pase. The ER reacted under such conditions, but the majority of the swollen Golgi cisternae did not. However, a few discrete elements were usually seen with significant deposits of reaction product. Fig. 11 shows a similar preparation of an SFV-infected cell treated with monensin. Again, while the ER clearly reacted uniformly, the ICBM structures were always free of reaction product.

THIAMINE PYROPHOSPHATASE (TPPase): This is a cytochemical marker for *trans* Golgi cisternae (21). In uninfected (Fig. 12) and infected (Fig. 13) BHK cells, as in other systems, one or two cisternae on one side of the Golgi stack specifically reacted for TPPase. In uninfected cells treated with monensin, only some of the swollen cisternae in the Golgi region were reactive. The majority of the cisternae, and all other organelles, did not react (Fig. 14). This clearly shows that despite the gross morphological changes the cytochemical individuality of the swollen cisternae was retained. When SFV-infected cells were treated with monensin and then reacted for TPPase, there was no reaction product in the ICBM structures (Fig. 16). The combination of SFV infection plus monensin treatment led to the appearance of a morphologically distinct structure in the Golgi region which reacted specifically and exclusively for TPPase (Figs. 15 and 16). This TPPase-positive structure appeared to comprise a rigid, fenestrated lamella, so convoluted as to form an approximately spherical shape. In negatively stained frozen sections (as well as in Epon sections, though less clearly) it was strikingly similar to insect septate junctions (17) with bridgelike structures being found across each cisterna, connecting the two membranes (Fig. 20). In oblique or transverse sections it was evident that these cross-bridges formed a periodic array (Fig. 20, *inset*). Although this structure may have had sparse deposits of reaction product for G-6-Pase (Fig. 11), they did not appear to be significant.

ACID PHOSPHATASE (AcPase): This is a cytochemical marker for lysosomal structures in many different cell types. It has also been used as a marker for *trans* Golgi cisternae, usually the most distal cisterna that has been referred to as a part of GERL (21). This cisterna has been shown to be continuous with parts of the lysosomal system.

In BHK cells, both before (Fig. 17) and after infection (not shown), there were variable amounts of reaction product in one or two cisternae on one side of the Golgi stack. There appeared to be some overlap with the TPPase-reactive cisterna, in that this cisterna sometimes had small but significant amounts of reaction product. Conversely, as is apparent in Fig. 13, the *trans*-most cisterna often contained significant deposits of lead when reacted for TPPase. The lysosomes were invariably positive for AcPase.

In the presence of monensin, BHK cells showed reaction product in lysosomes. It was not possible, however, to distinguish the latter from any reactive, swollen Golgi cisternae. When SFV-infected cells were treated with monensin, the same problem was evident but there was clearly no reaction product in ICBM structures (Fig. 18). Figs. 18 and 19 show reaction product in lysosomes. The reticular structure which always reacted for TPPase (Figs. 15 and 16) did not usually react for AcPase (Fig. 19), but occasionally some reaction product was seen (unpublished data). This again suggests that there is some overlap in the two cytochemical activities.

NICOTINAMIDE ADENINE DINUCLEOTIDE PHOSPHATASE (NADPase): Recent work by Smith (33) suggests that this enzyme activity might serve as a useful and specific cytochemical marker for Golgi cisternae in the middle of the stack. This activity was found by Smith (33) in rat incisor ameloblasts but we have unfortunately been unable to obtain a similar positive reaction using BHK cells.

CONTROLS FOR CYTOCHEMISTRY: In all cases the controls were negative.

Immunocytochemical Studies

Thin, frozen sections of infected BHK cells were labeled with RCA followed by anti-RCA antibodies and protein A–gold. We have previously shown (8) that this lectin labels up to three-quarters of the cisternae on the *trans* side of the Golgi stack. There were always one or two unlabeled cisternae on the *cis* side. An example is shown in Fig. 21. RCA labeling of infected cells treated with monensin showed gold particles over the plasma membrane, lysosomes, ICBMs, and the characteristic TPPase-reactive element as shown in Fig. 22. RCA labeling of the ICBMs appeared to be restricted to the membrane of these vacuoles and not associated with the membranes of the budding or budded viral particles. This was seen more clearly in double-label experiments in which bound RCA and

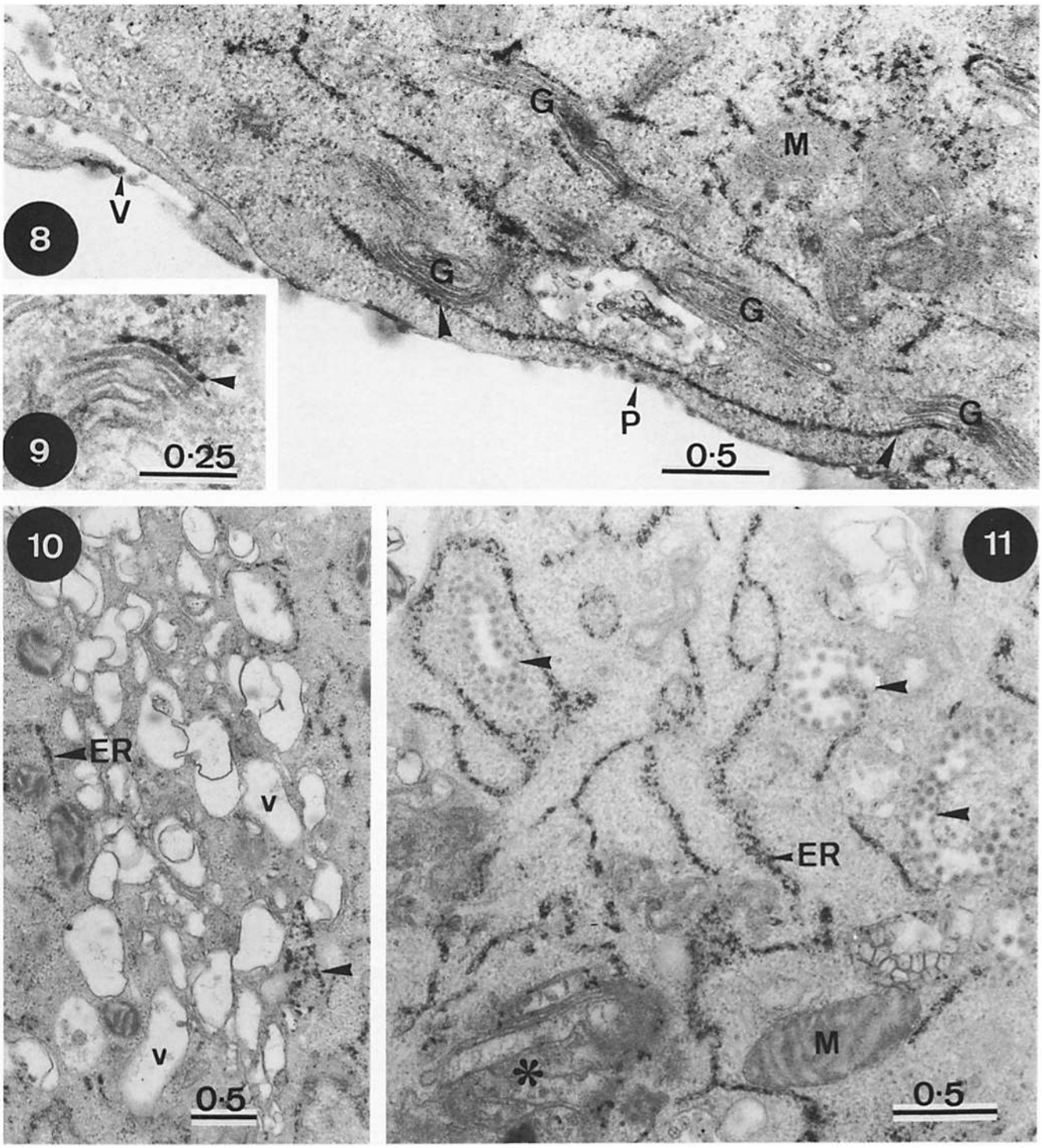

FIGURES 8–11 BHK cells reacted for G-6-Pase. In all cases the ER reacted positively. Figs. 8 and 9 are from SFV-infected BHK cells. The reactive ER clearly comes into close apposition to the Golgi stack (Figs. 8 and 9, arrowheads). In Fig. 8 the arrowheads indicate one sheet of *ER* which is contiguous to two widely separated Golgi stacks (*G*). It is very difficult to distinguish unequivocally between reaction product in true *cis* Golgi cisternae (as Fig. 9 might suggest) and close apposition of reactive *ER* with the Golgi stack. The central cisternae of the Golgi stack are free of reaction product. Fig. 10: A BHK cell treated with 10 μM monensin. All except one (arrowhead) of the vacuolar structures (*V*) are devoid of reaction product. Fig. 11 shows G-6-Pase reaction product in an infected cell treated with monensin. The *ER* is reactive but the ICBM structures (arrowheads) are not. The asterisk denotes the TPPase-reactive cisterna (cf. Figs. 15 and 16) which is essentially free of reaction product. Fig. 8, × 36,000. Fig. 9, × 56,000. Fig. 10, × 22,000. Fig. 11, × 37,000.

the spike proteins were distinguished using gold particles of different sizes. Virus budding from untreated infected cells was labeled by both sizes of gold (Fig. 23), whereas the viral particles in ICBMs were mostly labeled by that size of gold used to localize the spike proteins (Figs. 24–26); that size of gold used to localize bound RCA was generally restricted to the membranes of the ICBMs (Figs. 24–26). To confirm these observations, we quantitated the labeling in these double-label

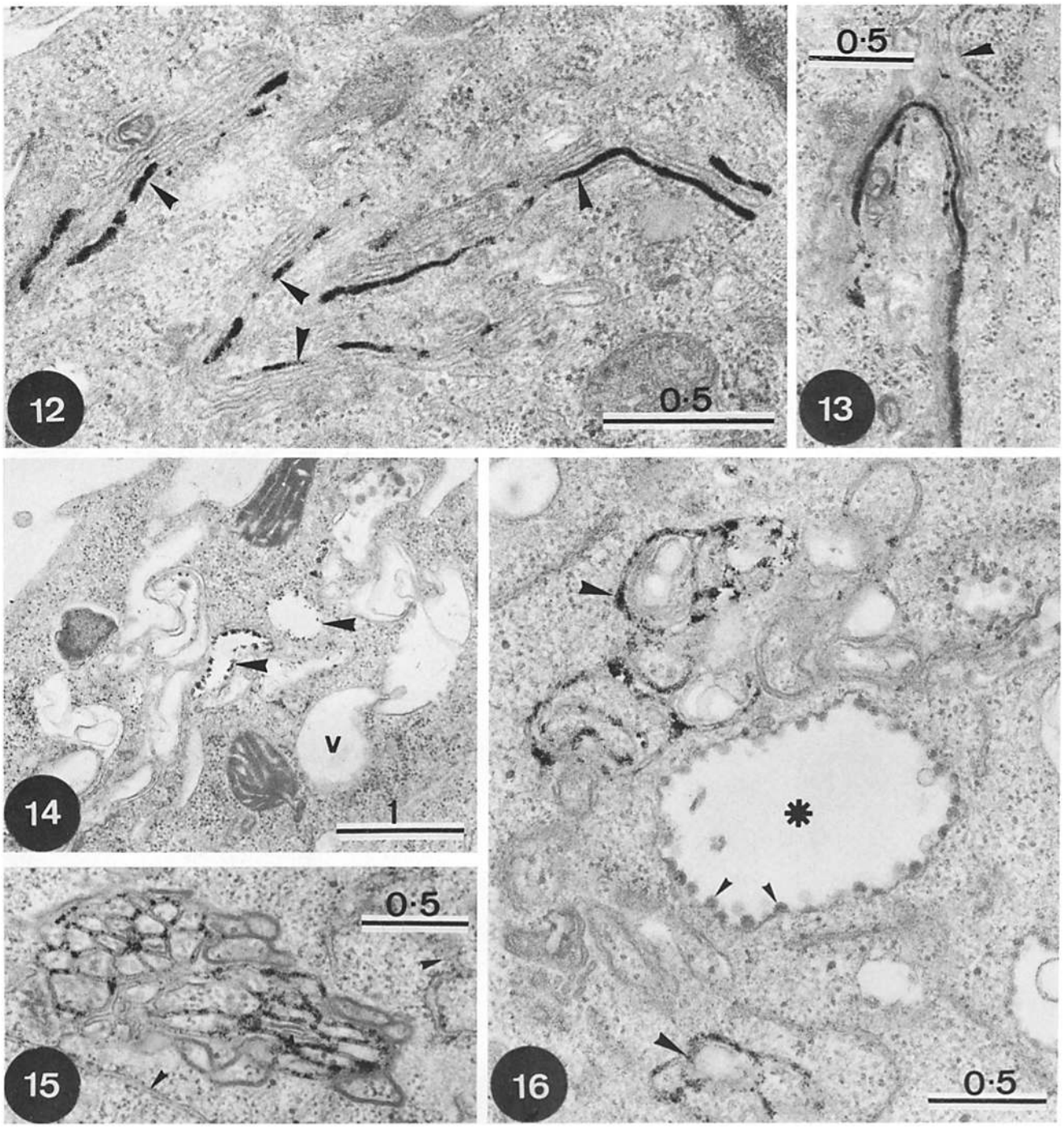

FIGURES 12–16 BHK cells reacted for TPPase. Fig. 12 is an image of a BHK cell, showing typical reaction product in one or two cisternae (arrowheads) on one side of the Golgi stack. This micrograph also indicates the difficulty in seeing any clear morphological difference between the two sides of the Golgi stack. Fig. 13 shows, in an SFV-infected BHK cell, a rare example where the ER adjacent to the obliquely sectioned Golgi stack (arrowhead) is free of ribosomes on the *cis* side of the Golgi stack, the one or two cisternae reactive for TPPase being located on the opposite side. Fig. 14 shows TPPase reaction product in two vacuoles (arrowheads) in a BHK cell after treatment with 10 μM monensin. The other vacuoles (*v*) are free of reaction product. Figs. 15 and 16 show BHK cells infected with SFV and treated with 10 μM monensin. In Fig. 15 the typical collapsed TPPase-positive cisterna is shown. Arrowheads indicate unreactive ER. In Fig. 16 the large arrowheads indicate parts of the TPPase-positive element. The ICBM (asterisk) has no reaction product. The small arrows within the ICBM indicate budding virions. Fig. 12, × 57,000. Fig. 13, × 34,000. Fig. 14, × 23,000, Fig. 15, × 34,000. Fig. 16, × 39,000.

experiments and the results are presented in Table I. Gold labeling of spike proteins was essentially the same whether the virus was budding from the plasma membrane of untreated cells or from the membrane of the ICBMs. In contrast, the level of RCA labeling of budding (or budded) virus in ICBMs was only one-third of that of virus budding from the cell surface. Furthermore, the RCA labeling of virus in ICBMs was to a large extent an unavoidable artifact of the method used to quantitate the labeling. Since all gold particles within 500 Å of the virus center were counted, gold particles labeling the ICBM

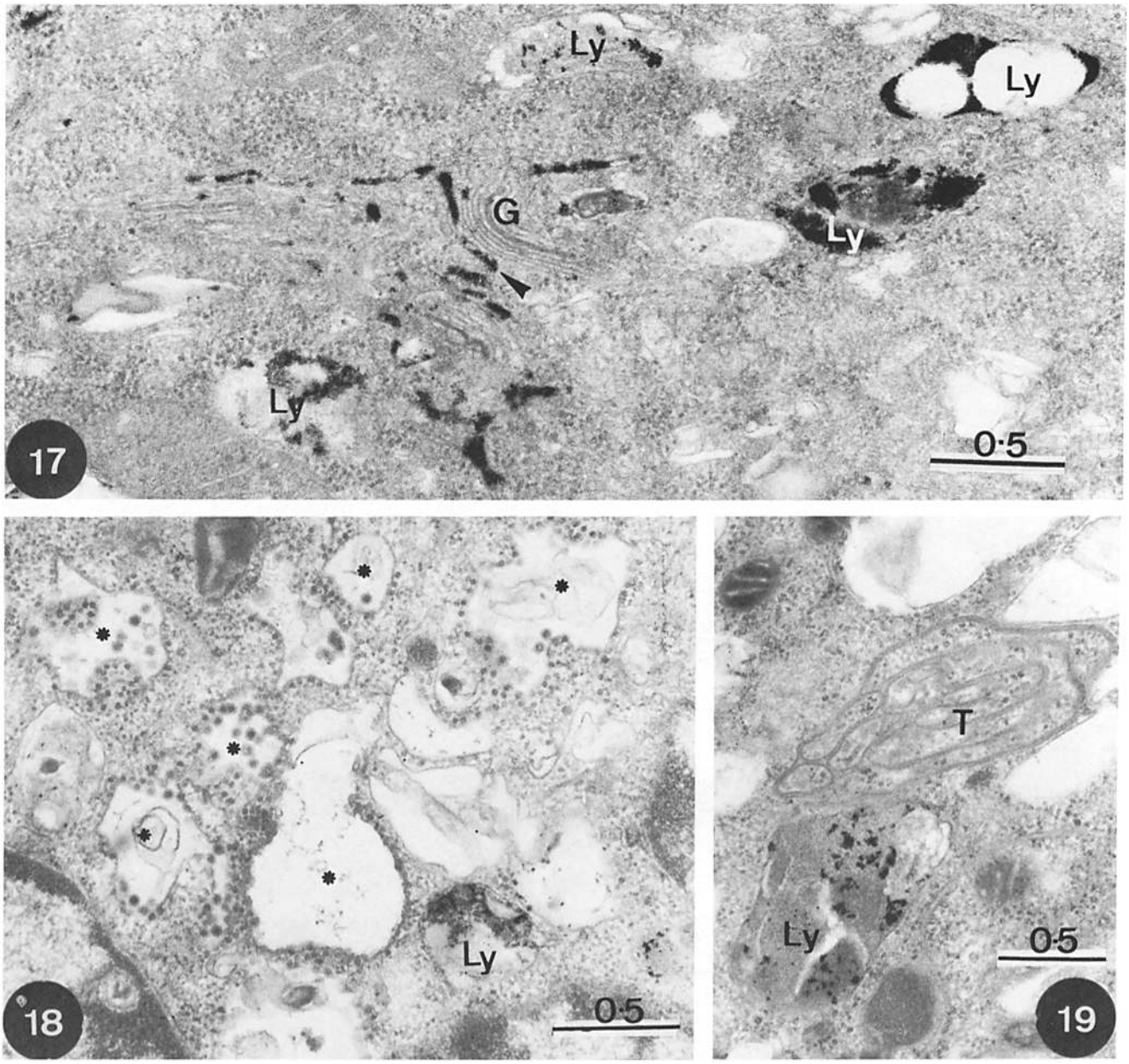

FIGURES 17–19 BHK cells reacted for AcPase. Fig. 17 shows typical reaction product in an uninfected cell. In the Golgi complex region (*G*), reaction product is found predominantly in one cisterna (arrowhead) on one side of the stack. Characteristically, a variable amount of reaction product is found in secondary lysosomes (*Ly*). Figs. 18 and 19 show the same reaction in SFV-infected cells treated with 10 μM monensin. In Fig. 18, the ICBMs (asterisk) are free of reaction product, whereas the *Ly* reacted. Similarly, in Fig. 19, whereas the *Ly* shows reaction product, the TPPase-reactive element (*T*) does not. Fig. 17, × 42,000. Fig. 18 × 34,000. Fig. 19, × 32,000.

membrane itself were necessarily included.

Double-labeling with RCA and anti-spike antibodies also allowed us to identify tentatively the *cis* Golgi compartment in infected cells treated with monensin. The cisternae comprising this compartment should be labeled by anti-spike antibodies but not by RCA, and an example is shown in Fig. 27. The level of labeling of these swollen cisternae was lower than that of the comparable *cis* cisternae in untreated cells, and their number was lower than expected. The reasons for this are not yet understood.

In summary, the ICBMs were labeled by a marker (RCA) which labels up to four cisternae on the *trans* side of the stack, but not by the cytochemical markers for the two *trans*-most cisternae. This evidence, in addition to a negative reaction with G-6-Pase, which labeled ER and possibly the first *cis* Golgi cisterna, would suggest that the ICBM structures are derived from one or two cisternae in the middle of the Golgi stack. We term these the ***medial*** cisternae.

VIRAL MEMBRANE PROTEINS IN ICBMs ARE UNCLEAVED AND UNTRIMMED

Labeling Studies with ^{35}S-Methionine

SFV-infected BHK cells were labeled for 5 min with ^{35}S-methionine and the proteins fractionated by SDS PAGE. After fluorography the two viral membrane proteins (E1 and p62) were clearly visible (Fig. 28, lane *1*). If the labeled cells were incubated for 90 min in the presence of excess unlabeled

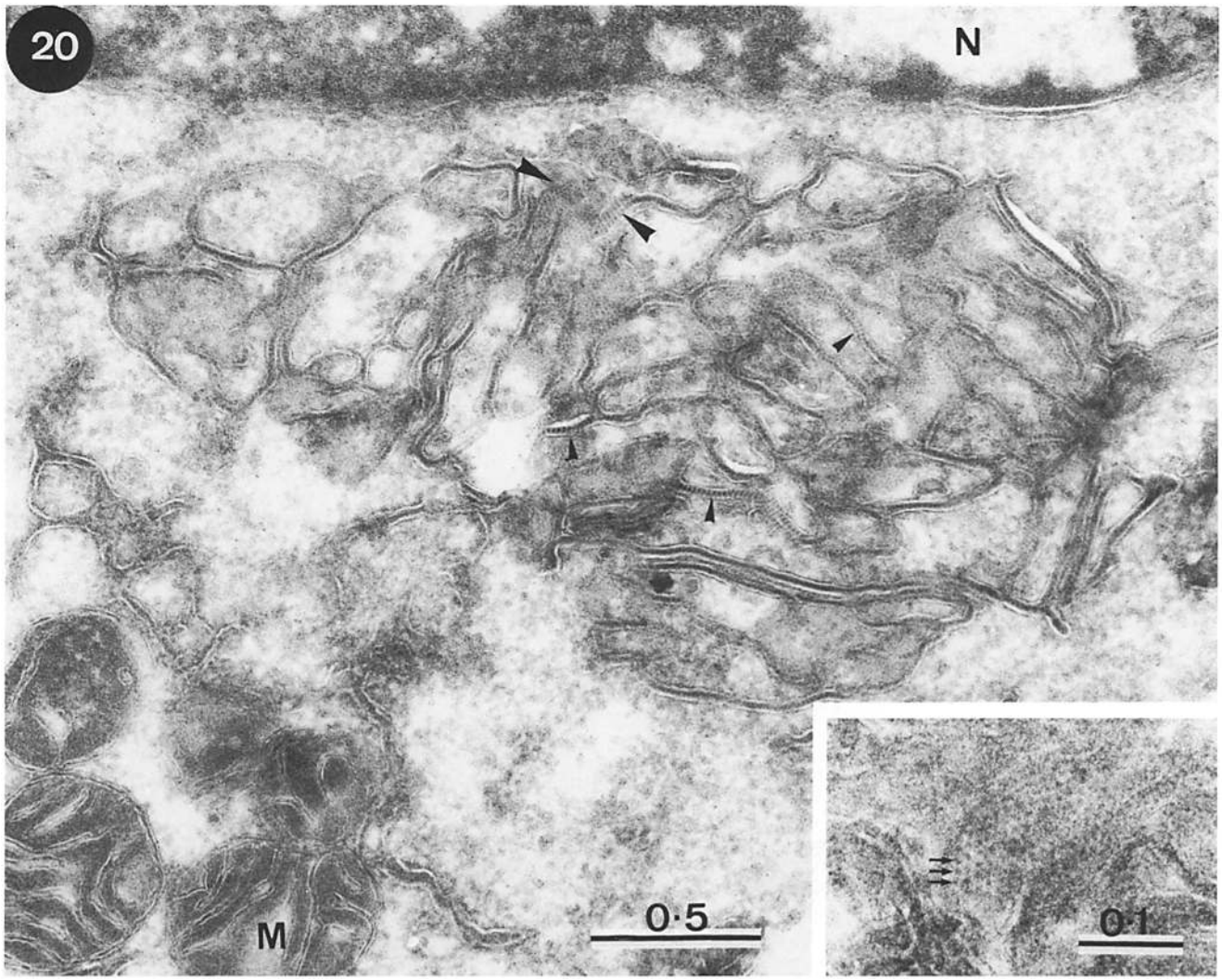

FIGURE 20 Frozen thin section of the TPPase-reactive element in a monensin-treated SFV-infected BHK cell. Although this section had been immunolabeled for RCA binding, the gold particles are hardly visible due to the heavy contrasting with uranyl acetate. However, this contrasting allows one to visualize periodic septate connections between the membranes of the flattened cisternae (small arrowheads). When cut transversely, this appears as a periodic array (large arrowheads). The *inset* shows this in greater detail. The arrows indicate the periodic repeat. × 48,000. *Inset*, × 148,000.

methionine, these viral membrane proteins were transported to the cell surface. During transport, E1 was converted to the mature form of higher molecular weight by the addition of terminal sugars (18) and p62 was cleaved to E2 (which co-migrates with mature E1) and E3 (not visible on this gel [see reference 5]) (Fig. 28, lane *2*). If 10 μM monensin was present during the 90-min incubation, neither of these changes occurred (Fig. 28, lane *3*). Since the maturation of E1 is an earlier biochemical event than the cleavage of p62 (5, 42), this suggests that monensin blocks transport before the addition of complex oligosaccharides.

The same experiments were carried out with a Ricin-resistant BHK line (Ric^R-14) which has <10% of the normal levels of *N*-acetylglucosaminyltransferase I (19). This cell line carries out the initial trimming of the mannose residues but is unable to complete trimming and then construct complex oligosaccharides. Immediately after labeling, the E1 and p62 migrated at the same rate as the proteins from BHK-21 cells (Fig. 28, lane *4*); during the 90-min incubation with excess unlabeled methionine, p62 was cleaved to E2 and E3 (not visible), and the mannose trimming caused the apparent molecular weight of E1 to decrease (Fig. 28, lane *5*). Since this decrease, as well as cleavage of p62, was prevented by monensin (Fig. 28, lane *6*), this suggests that monensin blocks before the high mannose oligosaccharides are trimmed.

Oligosaccharide Studies

To show directly that the high mannose oligosaccharides were not trimmed in the presence of monensin, we labeled infected BHK and Ric^R-14 cells for 15 min with [^{3}H]mannose and then incubated them for 90 min with excess unlabeled mannose in the presence or absence of monensin. The labeled viral proteins were exhaustively digested with proteinase K, and the resulting glycopeptides analysed by gel filtration both immediately and after further digestion with endoglycosidase H (Endo-H).

In the absence of monensin, the glycopeptides obtained varied with the host cell (Fig. 29 *a*). Endo-H treatment showed that in BHK-21 cells the oligosaccharides had been processed in part to give complex oligosaccharides, while in the Ric^R-14

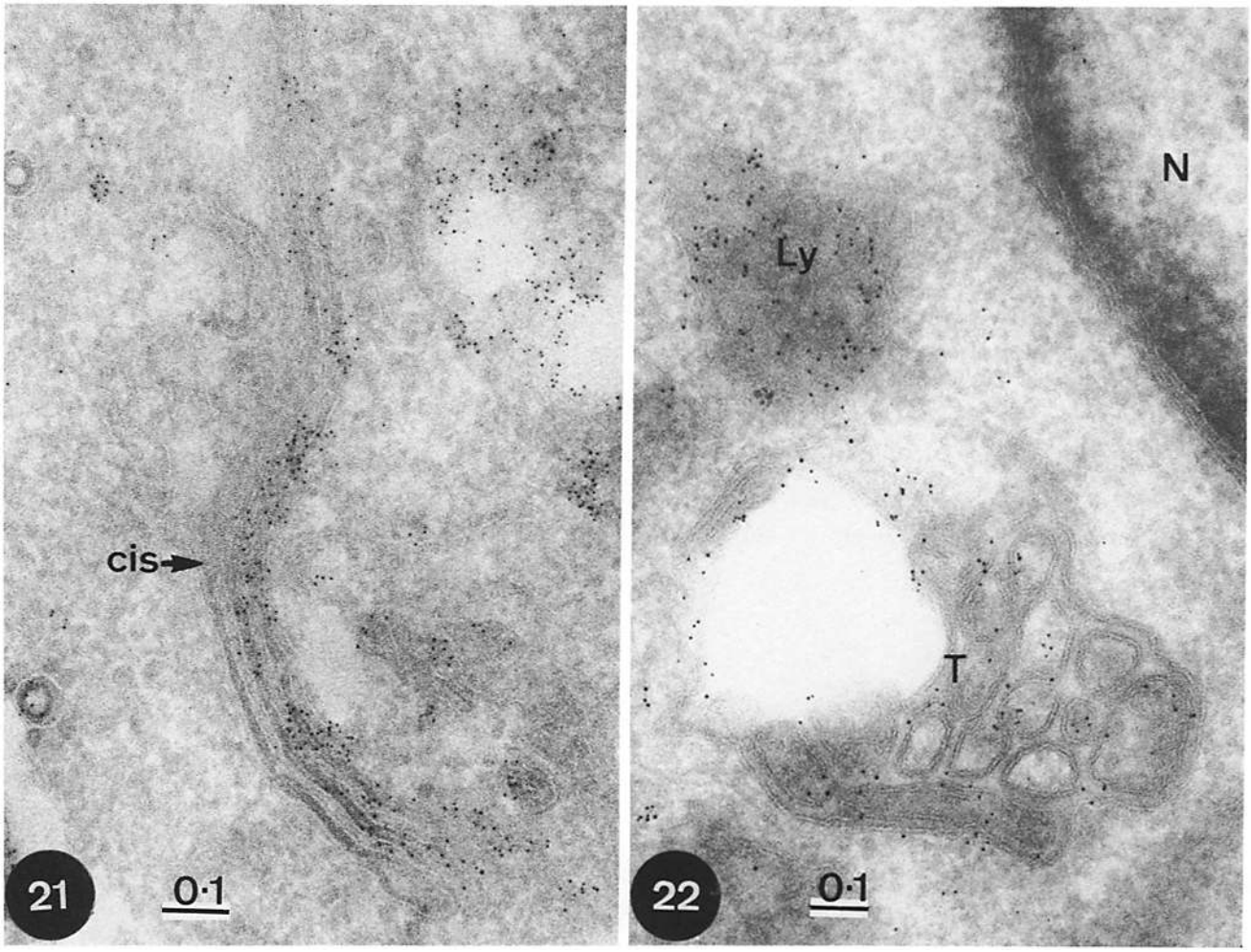

FIGURES 21–22 Frozen thin sections of SFV-infected BHK cells labeled with RCA followed by anti-RCA antibody and protein A-gold. Fig. 21 shows typical labeling of two cisternae on the *trans* side of the Golgi apparatus, leaving one cisterna on the *cis* side (*cis*) completely free of label. Fig. 22 shows a cell treated with 10 μM monensin. The characteristic TPPase-reactive element (*T*) labeled with RCA. A secondary lysosomelike structure (*Ly*) is also labeled. Fig. 21, × 89,000. Fig. 22, × 81,000.

cells all of the oligosaccharides remained Endo-H sensitive (Fig. 29 *b*).

Glycopeptides obtained from cells postincubated in the presence of monensin were of the same size regardless of whether the host cells were BHK-21 or Ric^R14 (Fig. 29 *c*). Treatment with Endo-H showed that in both cases the glycopeptides were of the Endo-H-sensitive, high-mannose type, and that no complex oligosaccharides had been constructed (Fig. 29 *d*). The elution position of the Endo-H released carbohydrate was compatible with removal of at most one mannose residue from the high-mannose oligosaccharide. The monensin block must therefore be before the lesion in the Ric^R14 cell line, and before the trimming step.

DISCUSSION

The data in this and the accompanying paper (27) can be explained most easily by assuming that the Golgi stack comprises a series of discrete compartments and that all copies of the viral membrane proteins must pass through each of them in turn. Transport between the compartments would probably be mediated by vesicles carrying the viral proteins (23). A schematic model for the functioning of the Golgi stack is depicted in Fig. 30 together with a detailed summary of the data. The evidence for this model is discussed below.

Monensin Treatment of SFV-infected BHK Cells Reveals Three Morphologically Distinct Golgi Compartments

In interpreting our data we assume that monensin does not affect the *functional identity* of the individual Golgi cisternae. It blocks transport of viral proteins between some of them, and this may be related to the drug-induced swelling and separation of the cisternae, but it does not, for example, cause random membrane fusion so that normally discrete Golgi functions are brought together in the same membrane compartment. This is most clearly seen after cytochemical staining for G-6-Pase, TPPase, or AcPase, or immunocytochemical labeling with RCA. Despite conversion by monensin of the Golgi stack into swollen vacuoles, approximately the same percentage of these vacuoles was stained or labeled as cisternae in the original intact Golgi stack. Assuming that the functional identity is retained in the presence of monensin, it is then possible to distinguish three distinct Golgi compartments. Each of these compartments would comprise one, or at most two, adjacent cisternae in any Golgi stack.

THE *cis* COMPARTMENT: These cisternae do not react positively for AcPase or TPPase and their membranes do not label with RCA in thin frozen sections. They may be positive

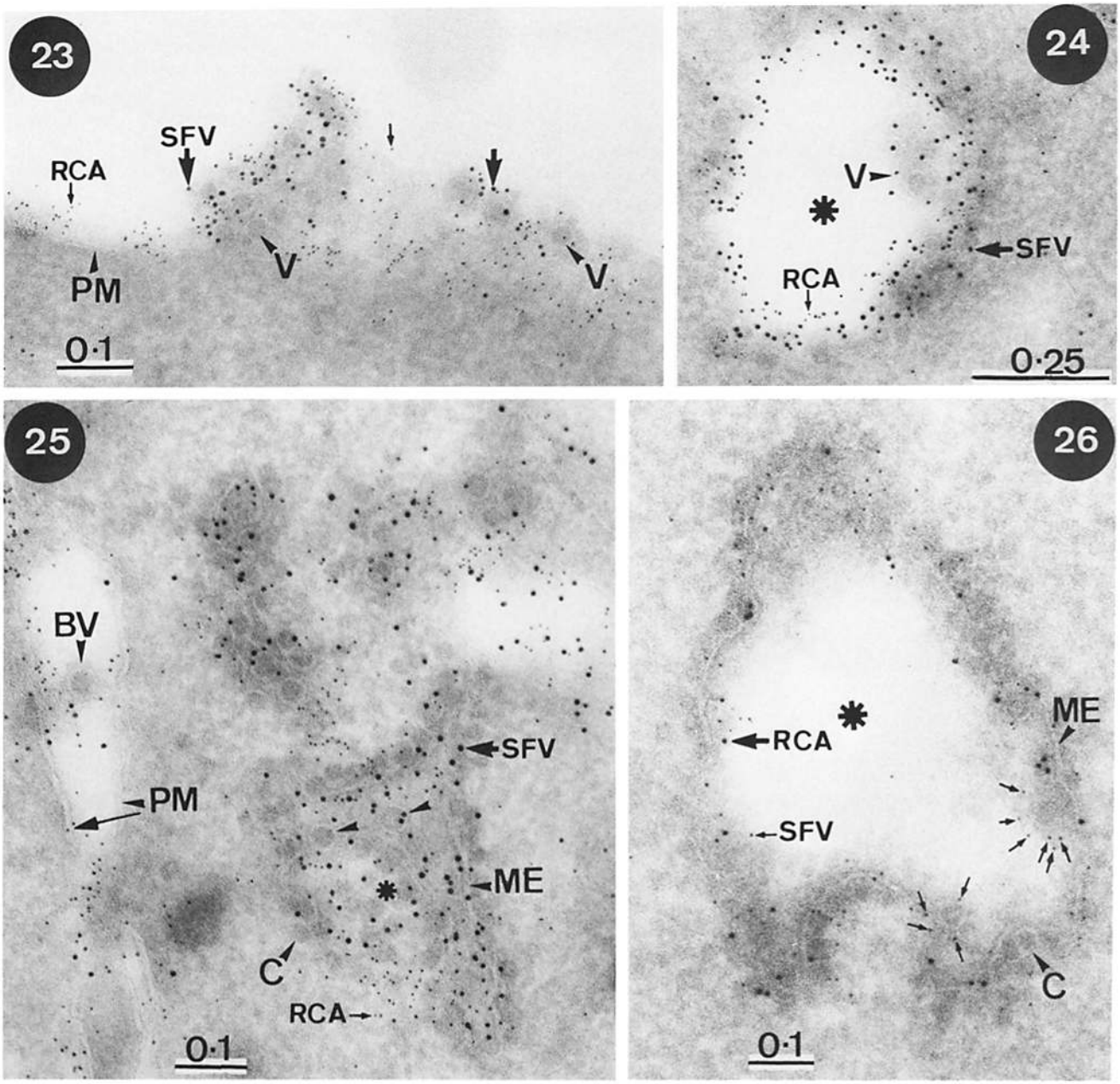

FIGURES 23–26 Frozen sections of infected BHK cells, double-labeled with antibodies to spike proteins and RCA. Fig. 23 shows labeling of the plasma membrane of an infected cell with antibody to RCA (5 nm gold, small arrows) and of virus particles (*V*) with antibody to spike proteins (12 nm gold, large arrow). Figs. 24–26 are of monensin-treated cells. ICBM structures (asterisks) were clearly labeled with both markers. In Figs. 24 and 25, anti-spike antibodies were labeled with 12 nm gold, RCA with 5 nm gold. In Fig. 24, a virus budded into the ICBM was labeled with five gold particles of 12 nm. Fig. 25 shows more clearly labeling of the ICBM compartment with both markers. The limiting membrane (*ME*) has capsids (*C*) on the cytoplasmic side. The arrowheads indicate virions budded into the ICBM which are mostly free of RCA (5 nm gold) labeling but are labeled with antibody to spike proteins (12 nm gold). At the plasma membrane (*PM*), labeling is predominantly with the 5 nm gold (anti-RCA). A budding virion, formed from spike proteins which have leaked through the monensin block, is indicated (*BV*). In Fig. 26, the labeling is reversed, RCA being visualized with 12 nm gold, and spike proteins with 5 nm gold. The ICBM membrane (*ME*) was labeled by both markers. Two budded virions were labeled only with 5 nm gold (small arrows). Fig. 23, × 117,000. Fig. 24, × 94,000. Fig. 25, × 100,000. Fig. 26, × 110,000.

for G-6-Pase but can be distinguished from G-6-Pase reactive ER since the latter is unaffected by monensin treatment. In infected cells they contain spike proteins at low concentrations, even in the presence of monensin, and bind few if any nucleocapsids.

THE *medial* COMPARTMENT: These cisternae do not react positively for TPPase, G-6-Pase, or AcPase but their membranes can always be labeled with RCA. In infected cells treated with monensin, the SFV membrane proteins accumulate in this compartment, causing nucleocapsids to bind in large numbers. They thus give rise to ICBMs. The fact that ICBMs do not stain for AcPase is important because it shows that they are not derived from the lysosomal system.

THE *trans* COMPARTMENT: This by definition reacts pos-

itively for TPPase and AcPase, and the membranes can also be labeled with RCA in thin, frozen sections. The TPPase-positive cisterna assumes a striking fenestrated appearance in infected cells treated with monensin and can be identified even in the absence of the TPPase reaction. The reasons for this appearance, and the periodic cross-bridges revealed in thin frozen sections, are unknown. Relatively low concentrations of SFV membrane proteins are found in these membranes in the presence of monensin, and occasional nucleocapsid binding is seen.

Different Golgi Functions Are Found in Different Compartments

Our data strongly suggest that monensin blocks the movement of SFV membrane proteins from the *medial* to the *trans* compartment. It also prevents the trimming of the high-mannose oligosaccharides bound to the viral proteins and the construction of complex oligosaccharides which is known to occur within the Golgi stack (5). These Golgi functions should therefore be restricted to the *trans* Golgi compartment. This is consistent with our previous work (8) and that of others, notably the recent work by Roth and Berger (29). They showed that one of the enzymes responsible for the construction of complex oligosaccharides, galactosyl transferase, co-localizes with TPPase in *trans* Golgi cisternae.

Covalent attachment of fatty acids to the viral membrane proteins was not blocked by monensin in this or in other viral systems (13). It is also an earlier event than construction of complex oligosaccharides (31). This would restrict fatty acylation to the *cis* or *medial* compartments. This has been confirmed by separating the *medial* compartments from the others on sucrose gradients as shown in the accompanying paper (27).

TABLE I

Quantitation of Double-labeling with RCA (Au5) and anti-SFV (Au12) over Budding and Budded Virus Particles *

	No. of gold particles/ viral profile	
Membrane	Anti-SFV	RCA
Plasma membrane of normal infected cells	10.5 ± 3.5	5.9 ± 2.9
ICBMs	8.1 ± 3.4	1.9 ± 1.5

* 50 budded virus profiles per count.

Viral Proteins Move from the cis to the medial to the trans Compartments

SFV membrane proteins appear to move from *cis* to *trans* Golgi cisternae (8). In this paper we provide strong evidence that monensin blocks the movement from the *medial* to the *trans* compartment. Since almost all of the viral proteins accumulate in the *medial* compartment (producing ICBMs), it is unlikely that there is movement directly from the *cis* to the *trans* compartment. It is reasonable to conclude that proteins in the *cis* compartment must move via the *medial* compartment to reach the *trans* one. This argues against a transport pathway, proposed for secretory proteins, which allows a product leaving the ER in a vesicle to enter any cisterna of the Golgi stack, or even bypass the Golgi stack altogether (23).

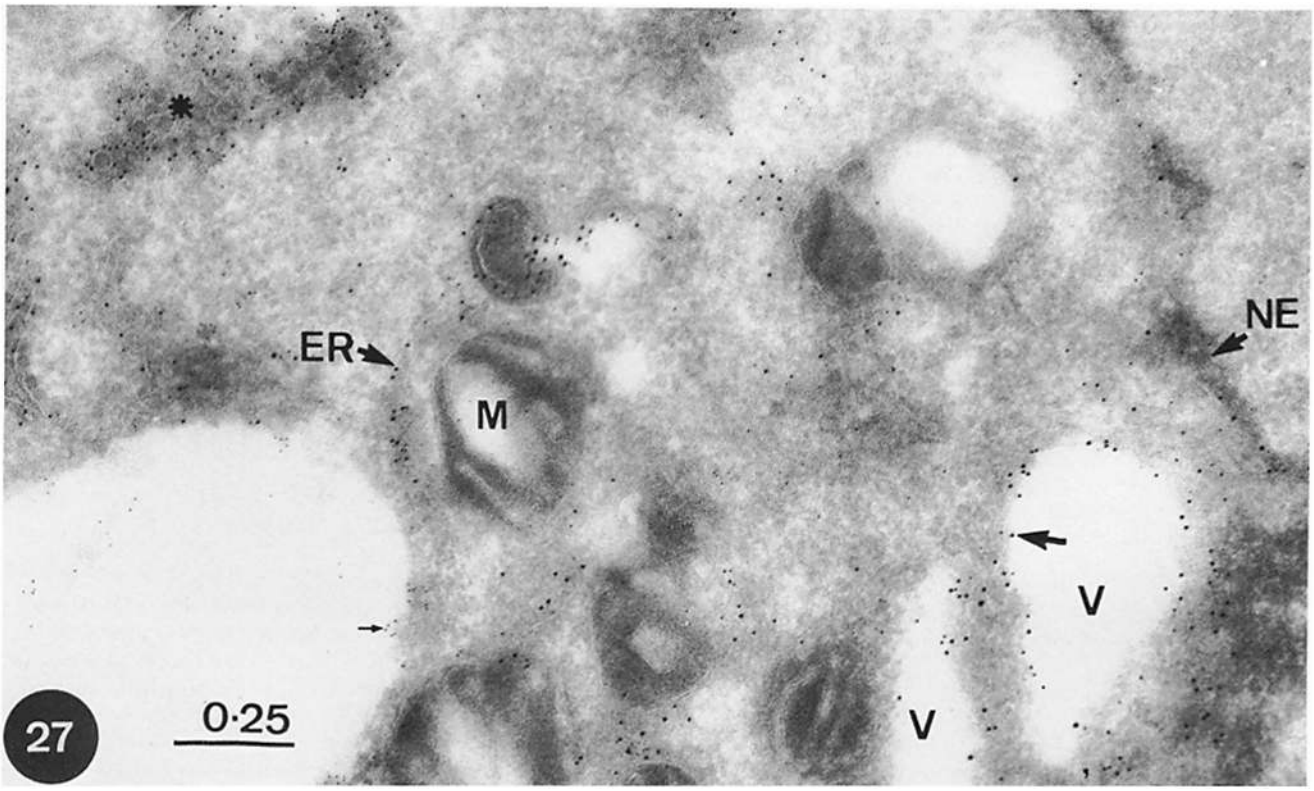

FIGURE 27 Frozen thin section of an infected BHK cell treated with 10 μM monensin and double-labeled with antibodies to spike protein, protein A (12 nm)-gold (large arrow) and RCA, anti-RCA antibodies and protein A (5 nm)-gold (small arrow). The ICBM structure (asterisk) was labeled with both antibodies, whereas the two vacuolar structures (*V*) adjacent to the nucleus were only labeled with anti-spike antibodies, as were the *ER* and nuclear envelope (*NE*). The large vacuole of unknown origin on the bottom left of the micrograph has reacted faintly with RCA (small gold) but is completely free of spike protein labeling. × 64,000.

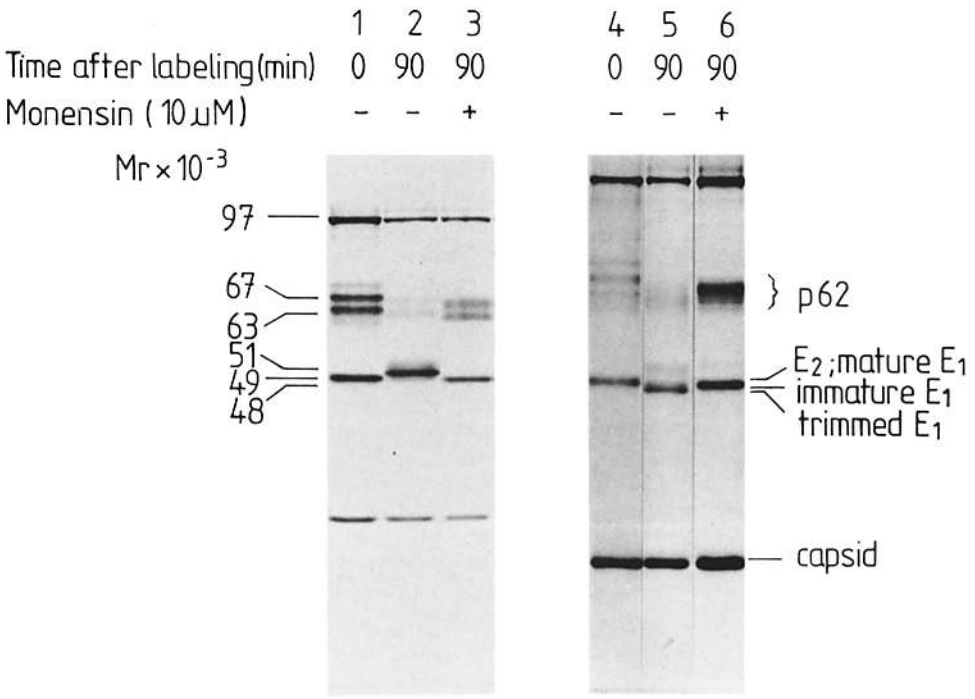

FIGURE 28 SDS PAGE of ^{35}S-methionine-labeled SFV-infected cells. The cell lines used were BHK-21 (lanes *1–3*) and Ric^R-14 (lanes *4–6*). Cells were labeled with ^{35}S-methionine for 5 min and harvested immediately (lanes *1* and 4) or subsequently incubated with excess unlabeled methionine for 90 min in the absence (lanes 2 and 5) or presence (lanes 3 and 6) of 10 μM monensin.

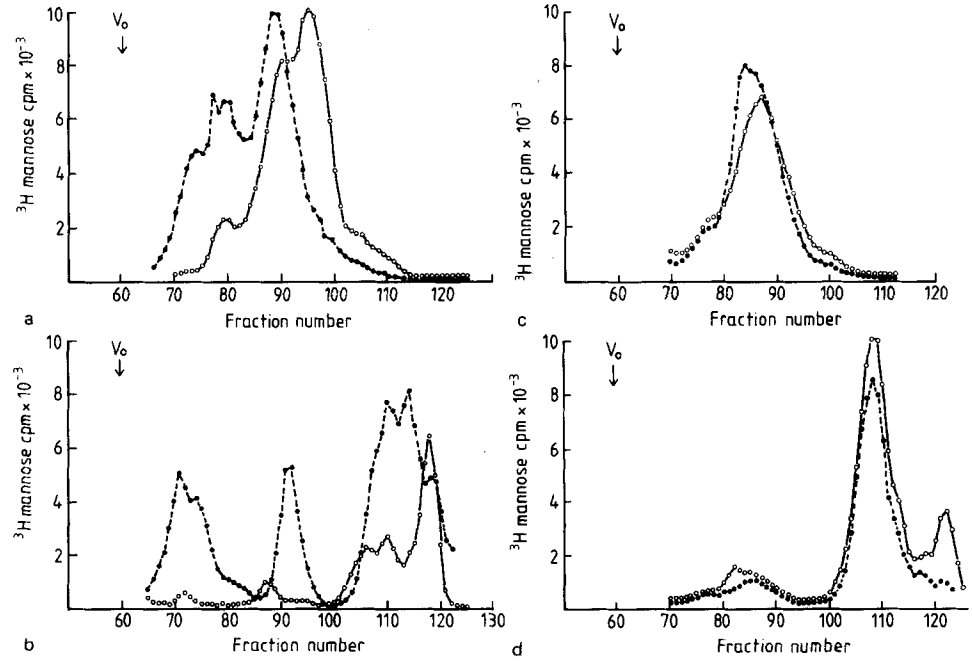

FIGURE 29 The oligosaccharides of SFV membrane proteins obtained from infected BHK-21 (●) or Ric^R-14 (○) cells. Fractionation was done by gel filtration on a Biogel P4 column. Glycopeptides were prepared from infected cells labeled with [^{3}H]mannose for 15 min, and then incubated with excess unlabeled mannose for 90 min. in the absence (a and b) or presence (c and d) of 10 μM monensin. The elution profiles are of the glycopeptides obtained before (a and c) and after (b and d) Endo-H digestion. V_o = void volume.

Recycling within the Golgi Complex

In SFV-infected BHK cells, RCA labels the *medial* and the *trans* Golgi compartments (8; and this paper). The RCA is bound to complex oligosaccharides, half of which are on transported viral proteins, the other half on endogenous Golgi components. Monensin blocks movement of the viral proteins to the *trans* compartment, where complex oligosaccharides are constructed. Yet the resultant ICBMs before the block were labeled by RCA which was recognizing the complex oligosaccharides on endogenous Golgi components. How had these endogenous components in the *medial* compartment acquired the complex oligosaccharides added in the *trans* compartment? The simplest explanation is that certain Golgi proteins must be involved in the transport of viral proteins between the *medial* and *trans* compartment. They would acquire complex oligosaccharides in the *trans* compartment when first synthesized and would then recycle to the *medial* compartment as they carry out their transport function.

Problems in the Use of Monensin as a General Tool

A note of caution must be added about the use of monensin. It blocks transport of material along a number of pathways, and the effects differ depending on the cell type and the

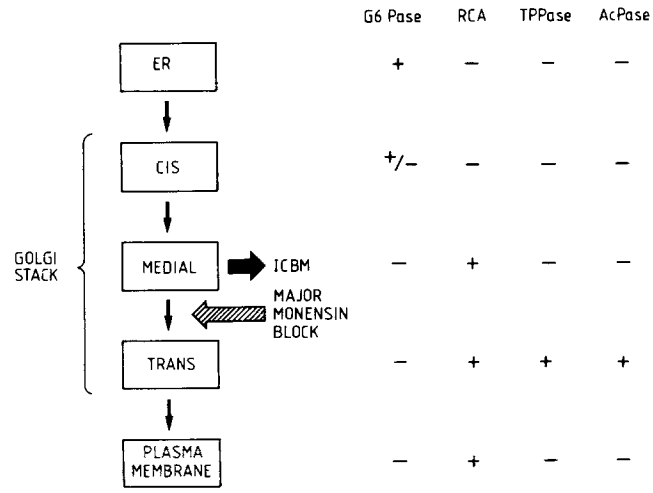

FIGURE 30 Schematic representation of compartments in the intracellular transport pathway and a summary of the cytochemical data obtained for SFV-infected BHK cells.

transported product (2, 32, 36, 37, 39, 41). It does not appear to be a specific drug, and results obtained in one system cannot necessarily be applied to another one. As a specific example and one which contrasts with the results presented here, consider chick embryo fibroblasts infected with SFV; monensin appears to block transport *after* the viral proteins have left the Golgi stack but before they reach the cell surface (24). For conclusions about its site of action and effects to be valid, a number of different approaches must be applied to a defined system as we have done here.

Another problem is the possibility of side-effects. One that might invalidate our interpretation of the data would be inhibition of the enzyme that trims mannose from the simple oligosaccharides, since the carbohydrate modifications observed during transport are not required for intracellular transport (6, 30). Inhibition of this enzyme would invalidate use of the carbohydrate modifications as a marker for the point reached by the transported proteins. The identification of the origins of the ICBMs would then rest on their labeling with RCA and lack of reaction for TPPase and AcPase; this would allow the possibility that ICBMs arise from fusion of post-Golgi vesicles. Fortunately, this particular possibility can be excluded as shown in the accompanying paper (27). After 2.5-min labeling with ^{3}H-palmitate, most of the labeled viral membrane proteins were found in the ICBM fraction. This compartment is therefore temporally very close to the *cis* Golgi, where fatty acid addition probably occurs (31), and must be within the Golgi stack, since viral membrane proteins need ~15 min to cross the Golgi stack (5).

In conclusion, we have determined the site at which monensin inhibits the transport of viral membrane proteins in SFV-infected BHK cells. This has allowed us to examine the pathway of transport, and to divide the Golgi stack into three distinct compartments. In the accompanying paper, we show that the unique physical properties of ICBMs can be exploited to distinguish them from the other Golgi compartments.

We thank Annemette Ohlsen and Ruth Giovanelli for excellent technical assistance; Dorothy Bainton, Steve Fuller, Karl Matlin, and Kai Simons for critical reading of the manuscript; Daniel Louvard for the anti-RCA antibodies; Dr. Hamill of Eli Lilly for the gift of monensin; Dr. Colin Hughes, National Institute for Medical Research, Mill Hill, London for the Ric^{R}-14 line of BHK cells; Keith Stanley for help with the acronym, ICBM; and Wendy Moses for typing the manuscript.

Received for publication 2 June 1982, and in revised form 3 November 1982.

REFERENCES

1. Acheson, N. H., and I. Tamm. 1967. Replication of Semliki Forest virus: an electron microscopic study. *Virology.* 32:128–143.
2. Basu, S. K., J. L. Goldstein, R. G. W. Anderson, and M. S. Brown. 1981. Monensin interrupts the recycling of low density lipoprotein receptors in human fibroblasts. *Cell.* 24:493–502.
3. Bergmann, J., K. Tokuyasu, and S. J. Singer. 1981. Passage of an integral membrane protein, the vesicular stomatitis virus glycoprotein, through the Golgi apparatus en route to the plasma membrane. *Proc. Natl. Acad. Sci. USA.* 78:1746–1750.
4. Farquhar, M. G., J. J. M. Bergeron, and G. E. Palade. 1974. Cytochemistry of Golgi fractions prepared from rat liver. *J. Cell Biol.* 60:8–25.
5. Green, J., G. Griffiths, D. Louvard, P. Quinn, and G. Warren. 1981. Passage of viral membrane proteins through the Golgi complex. *J. Mol. Biol.* 152:663–698.
6. Green, R. F., H. K. Meiss, and E. Rodriguez-Boulan. 1981. Glycosylation does not determine segregation of viral envelope proteins in the plasma membrane of epithelial cells. *J. Cell Biol.* 89:230–239.
7. Griffiths, G. W. 1979. Transport of glial cell acid phosphatase by endoplasmic reticulum into damaged axons. *J. Cell Sci.* 36:361–389.
8. Griffiths, G., R. Brands, B. Burke, D. Louvard, and G. Warren. 1982. Viral membrane proteins acquire galactose in *trans* Golgi cisternae during intracellular transport. *J. Cell Biol.* 95:781–792.
9. Griffiths, G., K. Simons, G. Warren, and K. T. Tokuyasu. 1982. Immunoelectron microscopy using thin, frozen sections: application to studies of the intracellular transport of Semliki Forest Virus spike glycoproteins. *Methods Enzymol.* In press.
10. Hubbard, S. C., and R. J. Ivatt. 1981. Synthesis and processing of asparagine-linked oligosaccharides. *Annu. Rev. Biochem.* 50:555–583.
11. Hubbard, S. C., and P. W. Robbins. 1979. Synthesis and processing of protein linked oligosaccharides *in vivo*. *J. Biol. Chem.* 254:4568–4576.
12. Hunt, L. A., J. R. Etchinson, and D. F. Summers. 1978. Oligosaccharide chains are trimmed during synthesis of the envelope glycoproteins of vesicular stomatitis virus. *Proc. Natl. Acad. Sci. USA.* 75:754–758.
13. Johnson, D. C., and M. J. Schlessinger. 1980. Vesicular Stomatitis virus and Sindbis virus glycoprotein transport to the cell surface is inhibited by ionophores. *Virology.* 103:407–424.
14. Kääriäinen, L., K. Hashimoto, J. Saraste, I. Virtanen, and K. Penttinen. 1980. Monensin and FCCP inhibit the intracellular transport of alpha-virus membrane glycoproteins. *J. Cell Biol.* 87:783–791.
15. Kornfeld, S., E. Li, and I. Tabas. 1978. The synthesis of complex oligosaccharides. II. Characterization of the processing intermediates in the synthesis of the complex oligosaccharide units of the vesicular stomatitis virus G protein. *J. Biol. Chem.* 253:7771–7778.
16. Krebs, H. A., and W. A. Johnson. 1937. The role of citric acid in intermediate metabolism in animal tissue. *Enzymologia.* 4:148–156.
17. Lane, N. J. 1974. Organisation of insect nervous system. *In* Insect neurobiology. J. E. Treherne, editor. North Holland Press, Amsterdam. 1–71.
18. Mattila, K., A. Luukonen, and O. Renkonen. 1976. Protein bound oligosaccharides of Semliki Forest Virus. *Biochim. Biophys. Acta.* 419:435–444.
19. Meager, A., A. Ungkitchanukit, R. Nairn, and R. C. Hughes. 1975. Ricin resistance in baby hamster kidney cells. *Nature (Lond.).* 257:137–139.
20. Meldolesi, J., N. Borgese, P. De Camilli, and B. Ceccarelli. 1978. Cytoplasmic membranes and the secretory process. *In* Membrane Fusion. G. Poste, and G. L. Nicholson, editors. Elsevier North Holland, Amsterdam.
21. Novikoff, A. B. 1976. The endoplasmic reticulum: a cytochemist's view (a review). *Proc. Natl. Acad. Sci. USA.* 73:2781–2787.
22. Novikoff, A. B., and R. Goldfisher. 1961. Nucleosidediphosphatase activity in the Golgi apparatus and its usefulness in cytological studies. *Proc. Natl. Acad. Sci. USA.* 47:802–810.
23. Palade, G. E. 1975. Intracellular aspects of the process of protein synthesis. *Science (Wash. DC).* 189:347–358.
24. Pesonen, M., and L. Kääriäinen. 1982. Incomplete complex oligosaccharides in Semliki Forest virus envelope proteins arrested within the cell in the presence of monensin. *J. Mol. Biol.* 158:213–230.
25. Pesonen, M., J. Saraste, K. Hashimoto, and L. Kääriäinen. 1981. Reversible defect in the glycosylation of the membrane proteins of Semliki Forest virus ts-1 mutant. *Virology.* 109:165–173.
26. Pressman, B. C. 1976. Biological applications of ionophores. *Annu. Rev. Biochem.* 45:501–530.
27. Quinn, P., G. Griffiths, and G. Warren. 1983. Dissection of the Golgi complex. II. Density separation of specific Golgi functions in virally infected cells treated with monensin. *J. Cell Biol.* 96:851–856.
28. Robinson, D. E. 1981. The ionic sensitivity of secretion-associated organelles in root cap cells of maize. *Eur. J. Cell Biol.* 23:267–272.
29. Roth, J., and E. G. Berger. 1982. Immunocytochemical localisation of galactosyl transferase in HeLa cells: codistribution with thiamine pyrophosphatase in *trans* Golgi cisternae. *J. Cell Biol.* 92:223–229.
30. Roth, M. G., J. P. Fitzpatrick, and R. W. Compans. 1979. Polarity of influenza and vesicular stomatitis glycoprotein maturation in MDCK cells: lack of requirement for glycosylation of viral glycoproteins. *Proc. Natl. Acad. Sci. USA.* 76:6430–6434.
31. Schmidt, M. F. G., and M. J. Schlesinger. 1980. Relation of fatty acid attachment to the translation and maturation of vesicular stomatitis and Sindbis virus membrane glycoproteins. *J. Biol. Chem.* 255:3334–3339.
32. Smilowitz, H. 1979. Monovalent ionophores inhibit acetylcholinesterase release from cultured chick embryo skeletal muscle cells. *Mol. Pharmacol.* 16:202–214.
33. Smith, C. E. 1980. Ultrastructural localisation of Nicotinamide Dinucleotide Phosphatase (NADPase) activity to the intermediate saccules of the Golgi apparatus in Rat incisor ameloblasts. *J. Histochem. Cytochem.* 28:16–26.
34. Tabas, I., S. Schlesinger, and S. Kornfeld. 1978. Processing of high mannose oligosaccharides on the newly-synthesized polypeptides of the vesicular stomatitis virus G protein and the IgG heavy chain. *J. Biol. Chem.* 253:716–722.
35. Tartakoff, A. M. 1980. The Golgi complex: crossroads for vesicular traffic. *Int. Rev. Exp. Pathol.* 22:228–251.
36. Tartakoff, A., D. Hoessli, and P. Vassalli. 1981. Intracellular transport of lymphoid surface glycoproteins. Role of the Golgi complex. *J. Mol. Biol.* 150:525–535.

37. Tartakoff, A., and P. Vassalli. 1977. Plasma cell immunoglobulin secretion. Arrest is accompanied by alterations in the Golgi complex. *J. Exp. Med.* 146:1332–1345.
38. Tartakoff, A., and P. Vassalli. 1978. Comparative studies of intracellular transport of secretory proteins. *J. Cell Biol.* 79:694–707.
39. Vladutiu, G. D., and M. C. Rattazzi. 1980. The effect of monensin on β-hexosaminidase transport in normal and I cell fibroblasts. *Biochem. J.* 192:813–820.
40. Wachstein, M., and E. Meisel. 1956. On the histochemical demonstration of glucose-6-phosphatase. *J. Histochem. Cytochem.* 4:592–596.
41. Wilcox, D. K., R. P. Kitson, and C. C. Widnell. 1982. Inhibition of pinocytosis in rat embryo fibroblasts treated with monensin. *J. Cell Biol.* 92:859–864.
42. Ziemiecki, A., H. Garoff, and K. Simons. 1980. Formation of the Semliki Forest virus membrane glycoprotein complexes in the infected cell. *J. Gen. Virol.* 50:113–123.